


# Parameter determination and evaluation of a Thévenin dynamic model for a li-ion cylindrical cell used in CubeSat applications

Diego Fernández-Arias<sup>1</sup> and Juan J. Rojas,<sup>1,2</sup> 

<sup>1</sup>Laboratorio Delta (DeltaLab), Costa Rica, diego.fernandeza08@gmail.com

<sup>2</sup>Instituto Tecnológico de Costa Rica, Costa Rica, juanrojas@itcr.ac.cr

**Abstract**— *The limited processing capacity of the lean satellites means that the indicators describing the general state of the cells that make up their power subsystem are rarely estimated. Such is the case of the SOC, whose estimation will be relevant for the control of this subsystem during the mission. Following the idea that these satellites seek a low cost, in this work, a cost-effective cyler was integrated to obtain the parameters of the cells. These were used as the input data of a Thévenin equivalent circuit model with one RC pair to obtain the estimated SOC. The Coulomb Counting method was chosen to calculate the real SOC from simulated data of the BIRDS mission. The results were evaluated and compared with simpler methods to demonstrate their accuracy. A mean absolute percentage error (MAPE) of 1.00337% was obtained, showing that the selected Thévenin model produced precise results without compromising processing power for other functions during the satellite mission.*

**Keywords**—lean satellite; electrical power system; state of charge; equivalent circuit model

## I. INTRODUCTION

Since the introduction of the CubeSat standard by the California Polytechnic University in 1999, small satellites have become the starting point for new players in the space sector. The original intention for the creation of the standard was to provide affordable access to space for universities; this was fully achieved, as in the period from 2013 to 2022 more than 200 academic institutions launched small satellites [1]. For many non-space fairing nations, that small satellite developed by a national academic institution was the first in their history, as was the case for Costa Rica with Batsú-CS1[2], a 1U CubeSat.

Nowadays, CubeSats are also used by governments and commercial companies to reduce the development cost of new technologies and scientific investigations because of their standard size, simple design, and fast development cycle [3].

The electrical power system (EPS) of a CubeSat takes care of power generation, storage, and distribution. Energy storage is required to operate the CubeSat during the eclipse period of the orbit, and it is typically achieved with secondary-type (rechargeable) batteries, which are composed of interconnected electrochemical cells. The 18650 (18 x 65mm) li-ion cylindrical cells have been the standard for most CubeSats; they are available as commercially off-the-shelf components (COTS) from different manufacturers and are used in most commercially available battery pack solutions as well [4].

In batteries, the SOC (state-of-charge) indicates the available capacity normalized concerning rated capacity and

SOH (state-of-health) indicates a way of calculating the aging process of the battery. The method for SOH calculation is not universally agreed, instead, it can be calculated using the decrease in capacity or the increase in the internal resistance of the battery that occurs with aging.

Alternatives like online parameter estimations are being recently used to identify the OCV, and after some steps obtain the SOC. The least-square methods and Kalman filters are some of the most popular parameter estimators [5]. However, these statistical methods will require high computational performance, and on a nanosatellite, the computer will be limited in size and processing power. Thus, part of this work sought to demonstrate that, for some selected simpler models, the results were closely similar to the satellite-simulated data, even with models that are not as robust and do not require as much processing performance.

The SOC is an indicator of the battery capacity and cannot be measured directly, but it can be estimated by different approaches, such as the Coulomb Counting method (CCM), which is simple and consists of integrating the battery current over time. This process is considered accurate only when the cell capacity and the initial state of charge are known [6,7], which is the case in this work. The CCM calculates the remaining capacity by estimating the charge that is transferred in or out of the cell [8]. This method is not adequate for SOC estimation of a CubeSat in orbit but can be used on the ground as a reference for other estimation methods. In LEO, the eclipse occurs approximately every ninety minutes, and, per year, the cells perform a total of 5000 to 5500 cycles [9].

The relationship to know the CCM is given by the equation (2), described later in this work. To estimate the SOC by this method, it is necessary to know the coulombic efficiency at a certain time, the input current at the same certain time, the sample period, and the total cell capacity. Those specific times required for the coulombic efficiency and the input current describe that the equation is in its discrete form. Although it is not the best way to estimate the SOC of orbiting CubeSats, Coulomb counting, when a restart mechanism is applied to it to reset the initial values, is sometimes the only viable option for doing so. [10]

The Space Systems Laboratory (SETECLab) of the Costa Rica Institute of Technology participated in the development of Batsú-CS1 and since then it has been committed to contributing to the community with open initiatives. Starting in 2022, SETECLab started a project to extract and share the parameters

of an equivalent circuit model that can be used to determine the SOC (state of charge) of the batteries that compose its small satellites.

To ensure that the power subsystem of the lean satellite will not compromise the mission, the SOC must be estimated to know the condition of the battery, but the battery management system (BMS) of the satellite does not usually report this information. Both current-based and voltage-based estimation methods present some disadvantages that make model-based estimations, such as electric circuit models (ECMs), more reliable options [11].

The processing power of the BMS on these lean satellites is very limited, so it was theorized that a simple Thévenin model would be sufficient to describe the cell behavior on this type of satellite. This was validated with real data from a simulated satellite orbit, to test the accuracy of the model. This choice will not compromise the processing on the CubeSats while providing estimates very close to reality, protecting the power system and the entire mission.

For reasons like those mentioned, the Thévenin Equivalent model with one RC pair was chosen, this model is shown in Figure 1.

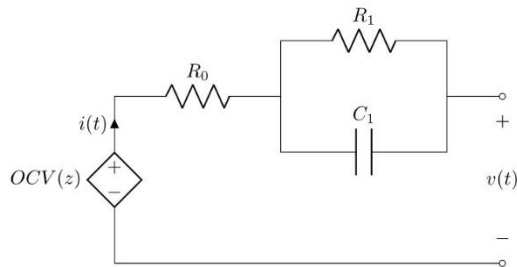


Figure 1. Thévenin ECM with one RC pair

As shown in Figure 1, the Thévenin model consists of the internal ohmic resistance in series with an RC pair. The resistance characterizes the instantaneous change in the charging and discharging process of the cell, while the RC characterizes the polarization effect of the cell while being used. This model is widely used because it is not excessively complex but still represents the static and dynamic behavior of the cell in an accurate way. Also, the process for obtaining the parameters has moderate difficulty [12,13].

However, despite being relatively simple and computationally straightforward, the Thévenin model has its limitations. Thus, for instance, with the increasing degree of battery aging, the accuracy of the SOC estimation based on this model decreases [14].

Furthermore, the Thévenin model will not describe conditions such as the hysteresis effect and the OCV variation due to the accumulation of the discharge current. Also, more complex models with more RC pairs should be used if more detailed terminal voltages are required, such as the GNL model [15].

An accurate estimation of the state of charge for lithium battery depends on accurately identifying of the battery model

parameters [12]. This work includes the recollection of parameters of the li-ion cells to create a dynamic model for SOC prediction and its respective validation in a lean satellite application. The MAPE was used to evaluate the precision of the obtained prediction.

At the core of this project was the development of a cell cycler. It consisted of an integration of both software and hardware, designed for the final purpose of repeatedly charging and discharging a li-ion cell.

## II. MATERIALS AND METHODS

To develop the model and validate its results, three steps contribute to the generation of the model: model selection, battery/cell testing, and model validation [18].

The first step of this work was the selection of the model, which was based on the application. In the case of lean satellite use, the charges and discharges given to the battery are dynamic but not as variable as in other applications. It is supposed that a dynamic Thévenin model is enough to describe the loads applied to the cells in a CubeSat. In the literature, many complex models are also used to describe this phenomenon, but they require more processing power because they have more variables to be monitored. In these satellites, this processing power is limited, so a Thévenin ECM can be sufficient to describe the cell behavior.

Next, to test the cells, some necessary parameters, which depend on the selected model, needed to be obtained. To make it, an experimental setting was required to start testing the cells, for which a cell cycler was integrated by combining different components. To gather these required values, long, constant charges were followed by other long and steady discharges. Then, discharge pulses at different C-rates were performed to obtain the last parameters. These were the capacity internal resistance  $R_0$ , resistance  $R_1$ , and capacitance  $C_1$  of the RC pair at different SOC. When this information was known, the model was ready to start computing its first results.

Once the cycler was finished, the first data sets were collected and used to verify that its control was correct. To achieve this, for instance, the cell capacity (Q) measurements for both charging and discharging were compared with the known Q provided by the manufacturer. Even though these capacities are not the same due to the internal cell resistance, they can be very similar if the charge/discharge rate is very small. The fact that these values were comparable made it possible to know that the measured data was correct.

Finally, the predictions from the Thévenin model were validated by comparing them with simulated data from a lean satellite in orbit. The real values of voltage and current were used to obtain the SOC of the cells of the satellite and see how it changed during the simulated orbit.

### A. Experimental setting

For the tests, several components were integrated to develop a cell cycler. Its purpose was to charge and discharge the cell to get the input data for the model. The cycler was



drop until it reached approximately 10% of the cell's Q. This indicated that now the discharging process was concluded.

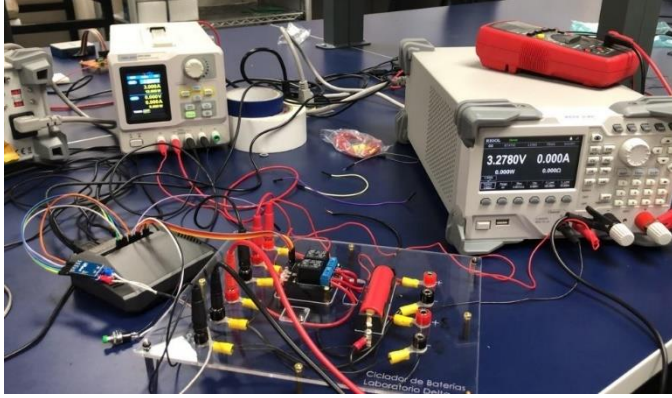


Figure 3. Li-ion cylindrical cell cycler

After the discharge process was completed, the FSM continued to its final step: the end state. The purpose of this last one was to finish the cycle. If, for example, the first cycle finished and the number of cycles entered as an input on the initial state was one, the program finished. If more than one cycle was required, the process started again until the current cycle number was equal to the requested in the initial state.

### C. Input parameters definition

The algorithm was originally designed to work with the Sanyo NCR18650GA cells. At the same time, it was intended to leave the opportunity to test the algorithm with other cylindrical li-ion cell chemistries. To do this, the input parameters of the algorithm can be changed at any given time, depending on the type of cell and its characteristics. These are the cell's nominal voltage, capacity, maximum charging voltage, minimum discharging voltage, and the maximum cell's surface temperature. Table 2 shows the values used. For this work, the temperature is going to be measured for safety purposes rather than input into the model. Defining these values depending on the chemistry used is key to ensuring that the future results of the battery cycling will correspond to the one that is being tested and to avoid safety hazards.

Table 2. NCR18650GA operational parameters

Specification	Value
Nominal voltage	3.6 V
Capacity	3450 mAh
Max. charging voltage	4.2 V
Min. discharging voltage	2.5 V
Max. temperature	60°C

### D. Data recollection

When the cycler was completed, the cells were charged and then discharged to gather the data. The voltage V, current I, capacity Q, and temperature T were measured and saved approximately every second. Another input of the model, which was not requested from the user but previously defined on the code, was the charge/discharge rate  $C_{rate}$ . For this work, a steady C/35 rate was defined so that abrupt changes that occur

at higher rates would not cause altered measurements. Since the li-ion cells tested in this experiment had an approximate 3500 mA h capacity when new, this meant that for a C/35 rate, 0.1 A flowed from the PS to the cell in the charging process, while 0.1 A flowed from the cell to the EL in the discharging process.

Before collecting the li-ion cell data, a pre-discharge was performed, ensuring that the tested cell would be fully discharged. The charging process started at almost the minimum discharging voltage, which is stated in Table 2. These theoretical values differed from the experimental, as seen in Table 3 and Table 4. Even though the pre-discharge took the cell to its minimum discharging voltage, the charging did not start at this exact moment. This was because the cell's voltage tended to stabilize towards its nominal voltage after being subjected to the charge/discharge. At this rate, a one-cycle complete charge of an NCR18650GA lithium-ion cell took almost 34 hours.

The data collected for the discharge stage is summarized in Table 4. The process started at nearly the maximum charging voltage and ended when the measured voltage reached the minimum discharging voltage. Another important detail is that even though the same  $C_{rate}$  of C/35 was used for both charging and discharging, the duration of both processes and the capacity were not the same.

Table 3. Cell values measured by the PS during the charging process

Seconds (s)	Voltage (V)	Current (A)	Capacity (mAh)	Temperature (°C)
0.18	2.731	0.1	0.01	18.25
1.19	2.74	0.1	0.03	20.5
2.19	2.745	0.1	0.06	18.5
3.2	2.748	0.1	0.09	20
4.2	2.751	0.1	0.12	18.25
⋮	⋮	⋮	⋮	⋮
123692.23	4.2	0.099	3435.89	18
123693.23	4.2	0.099	3435.92	19.5
123694.24	4.2	0.099	3435.95	18.75

Table 4. Cell values measured by the EL during the discharging process

Seconds (s)	Voltage (V)	Current (A)	Capacity (mAh)	Temperature (°C)
0.18	2.731	0.1	0.01	18.25
1.19	2.74	0.1	0.03	20.5
2.19	2.745	0.1	0.06	18.5
3.2	2.748	0.1	0.09	20
4.2	2.751	0.1	0.12	18.25
⋮	⋮	⋮	⋮	⋮
123692.23	4.2	0.099	3435.89	18
123693.23	4.2	0.099	3435.92	19.5
123694.24	4.2	0.099	3435.95	18.75

### E. Dynamic cell model

Once the capacity values for each given time and the experimental maximum capacity of the cell were obtained for both charge/discharge processes, it was possible to approximate the SOC for each time using (1).

$$SOC_k = 1 - \frac{Q_{[k]charge/discharge}}{Q_{maxcharge/discharge}} \quad (1)$$

To represent the dependence of the OCV on the SOC, the former needed to be defined. These values are equal to the measured voltage of the cell from Table 3 and Table 4.

After the SOC and OCV were known for every time, it was possible to know that the relationship between both variables is that the latter increased when the former also increased in the charge state, while in the discharge, the OCV decreased as the SOC of the cell went down. An average of these data between charging and discharging was sought to obtain final values to work with. As seen in Table 3 and Table 4, the number of data points is not the same for each data set. This meant that it was still not possible to look for an average between both processes' data.

To have the same amount of data, a linear interpolation was performed on each set to obtain, from all the data, 100 final values for both charging and discharging, so that now they could be averaged, as each set had the same amount of data. The result is represented in Figure 4. From now on, the OCV values that will be used for the model are the ones represented by the purple line.

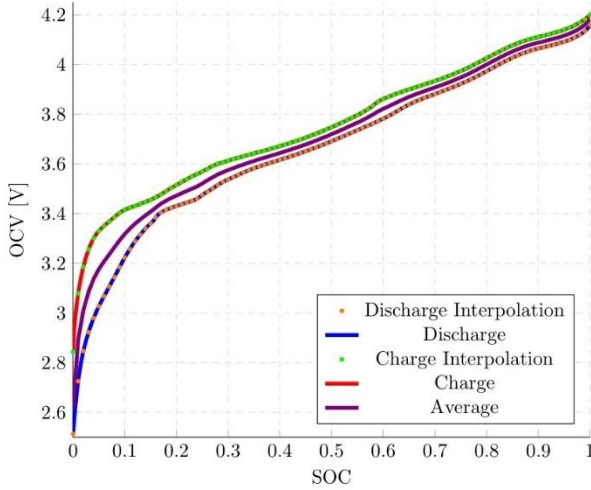


Figure 4. SOC vs OCV results for charge and discharge

Once the values of SOC and OCV to be worked with were known, the other parameters necessary to build the dynamic model were obtained. These are the cell's internal resistance  $R_0$  and  $R_1$  and  $C_1$  from the RC pair, which represents the polarization phenomenon of the cell [18].

A pulse discharge method was chosen to obtain the still missing parameters. For this one, the cell was discharged at a  $C_{rate} = 1C$  for 2 min. This time was chosen arbitrarily according to some previous laboratory tests because, with this time, the peak current drawn from the cell caused the cell voltage to drop easily appreciable and, after the 2 min, it will need considerable time to stabilize ( $\approx 5\tau$ ) to get to an updated OCV.

The proposed discharge method started with an initial standby for a minute. After this time passed, a constant discharge pulse, done by the electronic load, of 3.5 A started

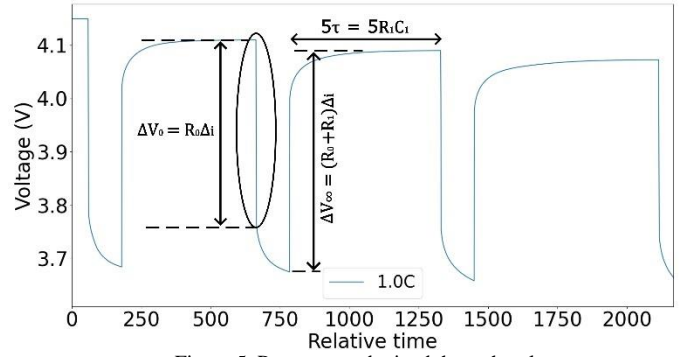


Figure 5. Parameters obtained through pulses

and remained constant for 2 min. Then, the load was disconnected, and the rest began. This state did not end when some arbitrary time passed. Instead, voltage values were measured every second for one minute to ensure that the cell voltage had stabilized before the next pulse was made. When the average of the voltage measured in that minute and the last voltage value measured in the previous minute were within 0.01% of each other, the voltage was considered to have stabilized, and the next discharge pulse was initiated. This process was carried out until it stopped when, in one of the discharges, the voltage reached the 2.5 V limit.

Figure 5 shows how the parameters were obtained from the discharge pulses. All the  $R_0$ ,  $R_1$ , and  $C_1$  were obtained for the 100 different SOC values.

The results of the discharge pulses, the values of the missing parameters, the construction of the model, and its validation can be seen in the results section.

#### E. Thévenin dynamic model construction

The parameters found in the previous section were the last information needed for constructing the Thévenin model.

The theoretical values of the SOC that were compared with the estimations were obtained using the CCM, represented in (2). It is important to consider that when a cell is fully charged, the SOC is 100%, while when fully discharged, it is 0%.

$$z[k+1] = z[k] - \frac{\Delta t}{Q} \eta[k] i[k] \quad (2)$$

Where  $z$  is another way used in the literature to represent the SOC. The  $\frac{i[k]\Delta t}{Q}$  part represents that, for a discrete time, the current is constant over time. Moreover,  $\eta[k]$  shows the coulombic efficiency and it is normally  $\eta[k] \leq 1$  during the charging process and  $\eta[k] = 1$  when discharging.

The next value obtained was that of the current passing through the resistance in the RC pair. To know it, it was assumed that the capacitor was fully discharged at the beginning, behaving as a short-circuit, which made  $i_{R_1}[0] = 0$ .

$$i_{R_1}[k+1] = e^{\left(\frac{-\Delta t}{R_1 C_1}\right)} i_{R_1}[k] + \left(1 - e^{\left(\frac{-\Delta t}{R_1 C_1}\right)}\right) i[k] \quad (3)$$

It was possible to predict the OCV values with the model parameters and the voltage and currents.

$$OCV_{predicted}(z[k]) = v[k] + R_1 i_{R_1}[k] + R_0 i[k] \quad (4)$$

These OCV values were used in inverse interpolation to finally obtain the SOC estimation based on this final equation.

$$z[k] \approx OCV^{-1}(v[k] + i[k]R_0) \quad (5)$$

If the initial estimate varied greatly from the real data, what happened was that the model needed some iterations to get more exact approximations. To reduce the error between the measurements and the theoretical values, the initial one of the first iteration was defined as  $SOC_{real} = SOC_{estimate}$ .

### III. RESULTS

The discharge pulses were executed at three different C-rate (0.5C, 1C, and 1.5C). During the first minute, the cell was in a rest state, so the measured Q was 0 mA h. The first and last measured parameters from one of the discharge pulses are observed in Table 5.

Table 5. Cell values measured by the EL during the discharging pulses at 1C

Seconds (s)	Voltage (V)	Current (A)	Capacity (mAh)	Temperature (°C)
0.18	2.731	0.1	0.01	18.25
1.19	2.74	0.1	0.03	20.5
2.19	2.745	0.1	0.06	18.5
3.2	2.748	0.1	0.09	20
4.2	2.751	0.1	0.12	18.25
⋮	⋮	⋮	⋮	⋮
123692.23	4.2	0.099	3435.89	18
123693.23	4.2	0.099	3435.92	19.5
123694.24	4.2	0.099	3435.95	18.75

The current stayed constant at 1C when discharging, while the voltage decreased until it reached the minimum discharging voltage. The discharge Q approached a value close to that of Table 4. The difference between these capacities was the rate at which the cell was discharged. The lower the C-rate at which the cell is tested, the closer the capacity will be to the actual Q provided by the manufacturer.

As shown in Figure 6, more pulses were applied to the cell before reaching the minimum value at a lower C-rate. This is because when an intense discharge was applied, such as those of 1C and 1.5C, the change in voltage during the 2-minute pulse duration was considerably greater. This caused the cell to need longer to stabilize its diffusion voltage and reach its new stable value ( $\approx 5\tau$ ).

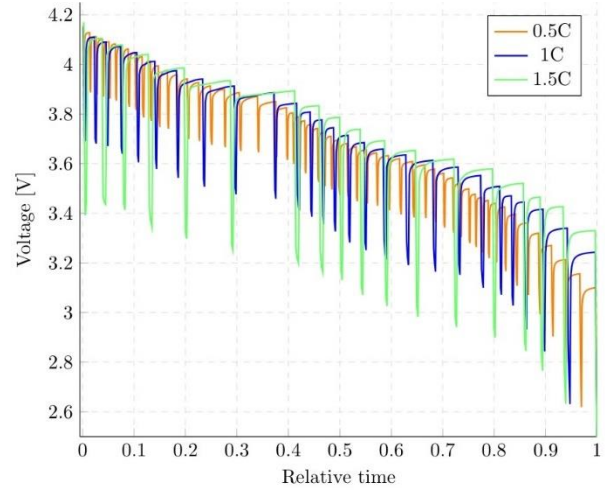
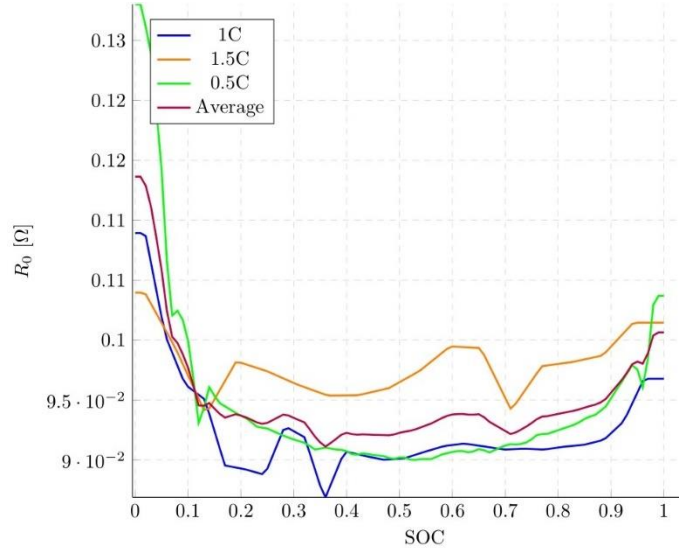
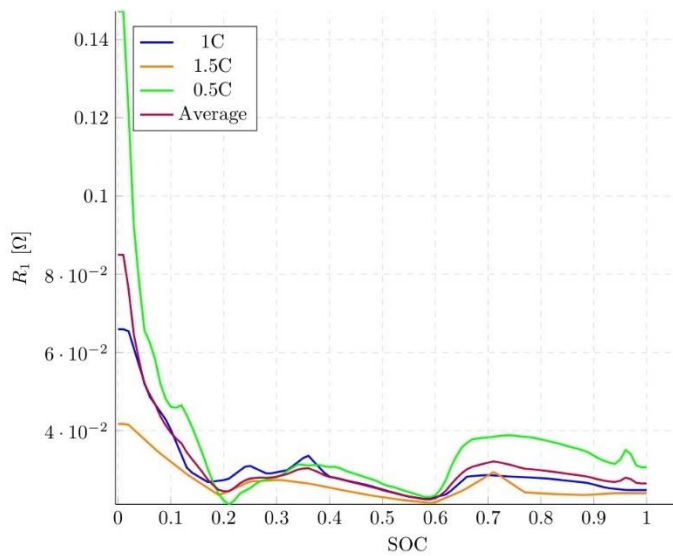


Figure 6. Cell voltage changes due to three different fixed applied currents

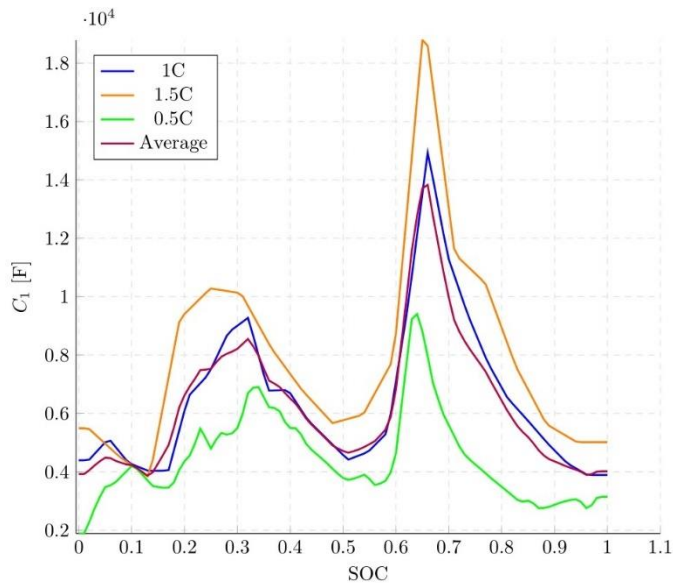
Each one of the three pulses had a different duration. For instance, at 0.5C, the discharge lasted nearly 13 hours, and at 1.5C, it lasted 5.5 hours. To directly compare the three series of pulses, it was necessary to normalize the time. This is why Figure 6 goes from 0 s to 1 s. The values of the  $R_0$ ,  $R_1$ , and  $C_1$  parameters depending on the SOC for each of the pulses are represented in Figure 7.



(a) SOC vs  $R_0$  at different  $C_{rates}$



(b) SOC vs  $R_1$  at different  $C_{rates}$



(c) SOC vs  $C_1$  at different  $C_{rates}$

Figure 7. Change in the parameters as SOC varies

To validate the information obtained from the cycling and the discharge pulses applied to the li-ion cells, it was necessary to have real data to compare. For this case, it was decided to take charge and discharge information from a dynamic application, i.e., its state of charge varied due to pronounced changes in the current that flowed through the cell. Thus, it was decided to use the information acquired from the cells of the power system that supplied energy to a lean satellite, which was equipped with external solar panels, throughout a simulated orbital period.

The fully regulated bus direct transfer (FRDET) architecture data of the lean satellite was taken as real values for the validation of the proposed dynamic model. With the tests performed on the satellite, the voltage and current were

obtained at any moment of the simulated orbital period, which had a duration of nearly 93 min. Throughout this time, two processes were distinguished: when the cell was supplying energy and the power was positive; the second one was when it was consuming and the power had negative values, as evidenced in Figure 8.

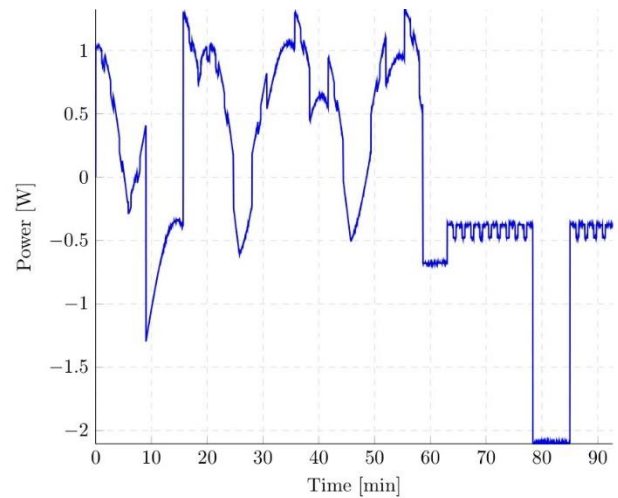


Figure 8. Replication of the power balance of a lean satellite cell to a  $V_{initial} \approx 4 V$  for the case of a FRDET power system architecture

For the original tests performed on the cell, more attention was given to the voltage, current, and power information than to the SOC. However, these variables could be calculated with the information summarized in Table 6. Note that these were the initial values used to calculate the actual SOC of the lean satellite cell for each instant with the CCM.

Table 6. Parameters to calculate the  $SOC_{real}$

$SOC_{initial}$	$\Delta t$ (s)	Capacity (mAh)	$\eta_{charge}$	$\eta_{discharge}$	$i$ (A)
0.77	1	3250	0.93	1	0.255

The  $\Delta t$ , capacity, and charge and discharge efficiencies ( $\eta$ ) were values given by the manufacturer. The calculated SOC values with the CCM, given by (2), were considered the real values with which the experimental data obtained in the laboratory were compared.

Knowing the power provided or consumed by the battery at every moment of the simulated orbital period, it was possible to reproduce the experiment with the NCR18650GA cell. To perform this replicate, the current and voltage were set at the EL and the PS, changing every second to ensure that the actual power profile was the same as the simulated one. The result can be seen in Figure 8. The cells used in the orbital period simulation were the Panasonic NCR18650B. They had a lower Q and a higher nominal voltage than the cells used for this work. The current and voltage values did not change, but the  $SOC_{initial}$  did as this value depends on the cell capacity, remembering from the CCM equation, and the cell's parameters, which vary depending on the cell's chemistry.

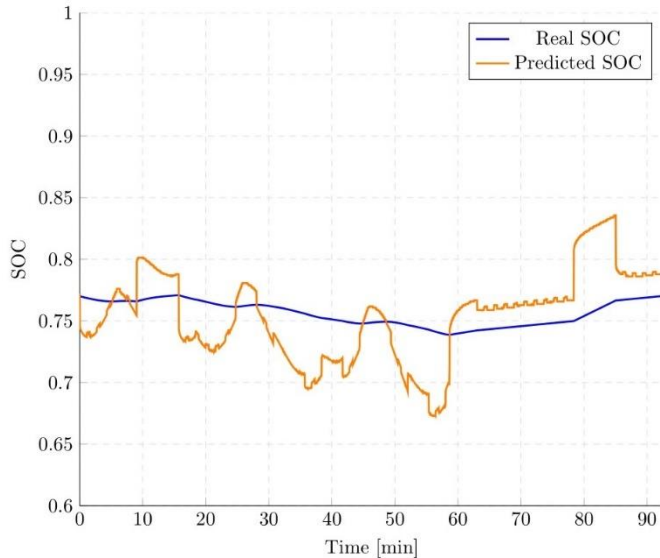
Therefore, the  $SOC_{initial_{real}}$  changed concerning the  $SOC_{initial_{predicted}}$ .

To know how close the predicted values will be to the real ones coming from the satellite measurements, the MAPE indicator was used to evaluate, which is defined as follows.

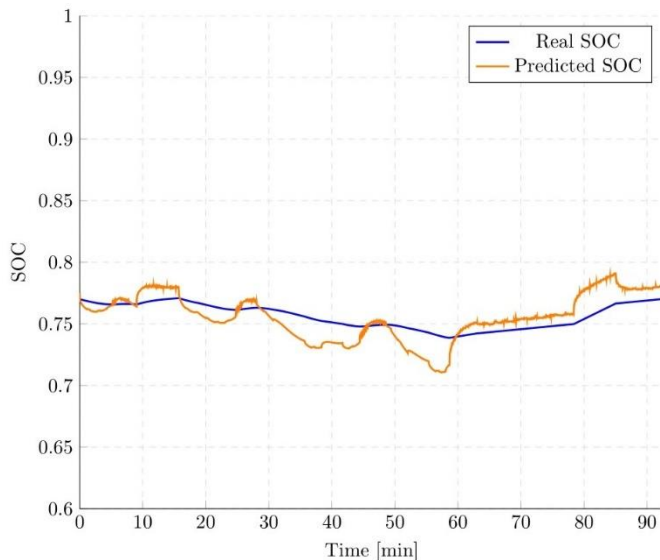
$$MAPE = \frac{1}{N} \sum_{k=1}^N \frac{|R_k - F_k|}{|R_k|} \times 100 \quad (6)$$

Where  $R_k$  is the real value and  $F_k$  is the predicted value.

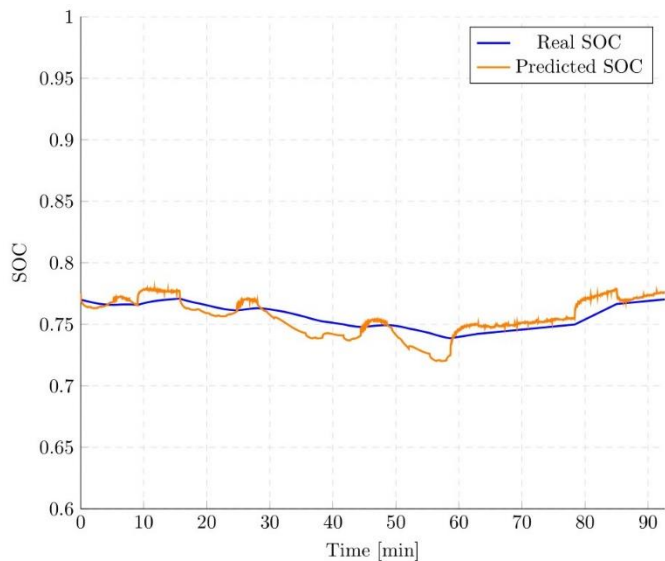
Figure 9 describe the predicted and real behavior of the SOC during the lean satellite simulated orbital period.



(a) Static model



(b)  $R_{int}$  model



(c) Thévenin model

Figure 9. Real and predicted SOC throughout the lean satellite simulated orbital period

The MAPE statistical indicator was used with three different models (one static and two dynamics) to observe how the results improved when passing from static to dynamic models and then, considering more variables, producing more robust ECMs. The results are summarized in Table 7.

Table 7. Errors in the three model predictions

Static MAPE (%)	$R_{int}$ MAPE (%)	Thévenin MAPE (%)
3.7708	1.4808	1.0037

#### IV. CONCLUSIONS

At the beginning of this work, it was theorized that the dynamic, but simple Thévenin model would estimate the SOC with precision and without compromising the processing power of the lean satellite. The selected statistical indicator confirmed the low error obtained with every one of the models.

In future research, the hysteresis effect will be considered during the experiments to reduce the error. Also, performing the characterization of the cells at different controlled temperature profiles is considered for future work. As of now, a cost-effective temperature-controlled chamber for cells is being fabricated to replicate the rapidly changing temperature working conditions.

#### ACKNOWLEDGMENT

The authors would like to thank the DELTA laboratory of the Instituto Tecnológico de Costa Rica and its collaborators.

#### REFERENCES

- [1] BryceTech. Smallsats by the Numbers, 2023.
- [2] Jenkins, M.G.; Calvo-Alvarado, J.C.; Calvo-Obando, J.; Jimenez, A.C.; Carvajal-Godinez, J.; Valverde, A.; Molina, J.C.R.; Rosales, L.C.; Martinez, E.; Jimenez-Salazar, V.; Monge, L.D.; Alvarado, C.; Rojas, J.J.; Hernandez, M. Testing and Operations of a Store and Forward CubeSat for Environmental Monitoring of Costa Rica. 69th International Astronautical Congress 2018, 2018.



- [3] NASA. CubeSat Launch Initiative Overview and CubeSat 101, 2017.
- [4] NASA. State of the Art Small Spacecraft Technology; National Aeronautics and Space Administration, 2022.
- [5] Knap, V.; Stroe, D.I. Effects of open-circuit voltage tests and models on state-of-charge estimation for batteries in highly variable temperature environments: Study case nano-satellites. *Journal of Power Sources* 2021, 498, 229913. doi:<https://doi.org/10.1016/j.jpowsour.2021.229913>.
- [6] Movassagh, K.; Raihan, A.; Balasingam, B.; Pattipati, K. A Critical Look at Coulomb Counting Approach for State of Charge Estimation in Batteries. *Energies* 2021, 14. doi:[10.3390/en14144074](https://doi.org/10.3390/en14144074).
- [7] Fathoni, G.; Widayat, S.A.; Topan, P.A.; Jali, A.; Cahyadi, A.I.; Wahyunggoro, O. Comparison of State-of-Charge (SOC) estimation performance based on three popular methods: Coulomb counting, open circuit voltage, and Kalman filter. 2017 2nd International Conference on Automation, Cognitive Science, Optics, Micro Electro-Mechanical System, and Information Technology (ICACOMIT), 2017, pp. 70–74. doi:[10.1109/ICACOMIT.2017.8253389](https://doi.org/10.1109/ICACOMIT.2017.8253389).
- [8] Murmane, M.; Ghazel, A. A Closer Look at State of Charge (SOC) and State of Health (SOH) Estimation Techniques for Batteries, 2017. 9. Hill, C.A. Satellite battery technology — A tutorial and overview. *IEEE Aerospace and Electronic Systems Magazine* 2011, 26, 38–43. doi:[10.1109/MAES.2011.5936184](https://doi.org/10.1109/MAES.2011.5936184).
- [9] Hill, C.A. Satellite battery technology — A tutorial and overview. *IEEE Aerospace and Electronic Systems Magazine* 2011, 26, 38–43. doi:[10.1109/MAES.2011.5936184](https://doi.org/10.1109/MAES.2011.5936184).
- [10] Gregory Plett, *Battery Management Systems, Volume II: Equivalent-Circuit Methods*, Artech, 2015.
- [11] Aung, H.; Soon, J.J.; Goh, S.T.; Lew, J.M.; Low, K.S. Battery Management System With State-of-Charge and Opportunistic State-of-Health for a Miniaturized Satellite. *IEEE Transactions on Aerospace and Electronic Systems* 2020, 56, 2978–2989. doi:[10.1109/TAES.2019.2958161](https://doi.org/10.1109/TAES.2019.2958161).
- [12] Zhang, L.; Wang, S.; Stroe, D.I.; Zou, C.; Fernandez, C.; Yu, C. An Accurate Time Constant Parameter Determination Method for the Varying Condition Equivalent Circuit Model of Lithium Batteries. *Energies* 2020, 13. doi:[10.3390/en13082057](https://doi.org/10.3390/en13082057).
- [13] Barletta, G.; DiPrima, P.; Papurello, D. Thévenin’s Battery Model Parameter Estimation Based on Simulink. *Energies* 2022, 15. doi:[10.3390/en15176207](https://doi.org/10.3390/en15176207).
- [14] K. Huang, Y. Wang and J. Feng, "Research on equivalent circuit Model of Lithium-ion battery for electric vehicles," 2020 3rd World Conference on Mechanical Engineering and Intelligent Manufacturing (WCMEIM), Shanghai, China, 2020, pp. 492-496, doi:[10.1109/WCMEIM52463.2020.00109](https://doi.org/10.1109/WCMEIM52463.2020.00109).
- [15] Meng, Jinhao & Luo, Guangzhao & Ricco, Mattia & Swierczynski, Maciej & Stroe, Daniel-Ioan & Teodorescu, Remus. (2018). Overview of Lithium-Ion Battery Modeling Methods for State-of-Charge Estimation in Electrical Vehicles. *Applied Sciences*. 8. 659. [10.3390/app8050659](https://doi.org/10.3390/app8050659).
- [16] Crain, L. Equivalent Circuit Model Generation for Batteries Using Non-ideal Test Data. Master of science, Department of Engineering, University of Wisconsin-Milwaukee, 2018.
- [17] Castillo-Ocaña, G. Diseño y Construcción de un Ciclador de Baterías. *Tecnia* 2021, 31, 10 – 17. doi:[10.21754/tecnia.v21i1.1101](https://doi.org/10.21754/tecnia.v21i1.1101).
- [18] Gregory Plett, *Battery Management Systems, Volume I: Battery Modeling*, Artech, 2015.